Molecular spectra in collective Dicke states

Eran Sela,[1] Victor Fleurov,[1] and Vladimir A. Yurovsky[2]
[1]*Raymond and Beverly Sackler School of Physics and Astronomy, Tel Aviv University, Tel Aviv 6997801, Israel*
[2]*School of Chemistry, Tel Aviv University, Tel Aviv 6997801, Israel*
(Received 8 May 2016; published 26 September 2016)

We introduce a model describing the competition of interactions between N two-level systems (TLSs) against decoherence. We apply it to analyze dye molecules in an optical microcavity, where molecular vibrations provide a local source for decoherence. The most interesting case is when decoherence strongly affects each individual TLS, e.g., via broadening of emission lines as well as vibrational satellites; however, its influence is strongly suppressed for large N due to the interactions between TLSs. In this interaction-dominated regime we find unique signatures in the emission spectrum, including strong $O(\sqrt{N})$ level shifts, as well as $1/N$ suppression of both the decoherence width and the vibrational satellites. These effects are most pronounced in the unexplored regime near 50% polarization of the TLSs.

DOI: 10.1103/PhysRevA.94.033848

I. INTRODUCTION

The dynamics of quantum two-level systems (TLSs) has always been at the focus of interest, but recently, it has attracted increased attention because of ideas of quantum computing [1]. A crucial requirement is the preservation of phase coherence in the presence of a noisy *environment*. The resulting spin-boson models have been extensively studied (see the reviews [2,3]). In many systems the *interactions* between TLSs lead to collective behavior, such as Dicke superradiance [4].

In this article we describe the competition between local decoherence, on the one hand, and interaction between N TLSs (see Fig. 1), on the other. We consider molecules in a two-dimensional optical microcavity. A TLS excitation may hop between molecules via emission and absorption of virtual cavity photons. These are effectively two-dimensional massive bosons [5], and as a result, the interaction acquires a finite length scale ℓ [6]. In this paper we assume that there is a large number N of molecules within this interaction range (see [7,8]).

As a starting point, we observe that as a result of interactions, the ground state becomes a large quantum superposition of states with a given total number of excited TLSs $N_{\rm ex} \leqslant N$ coherently shared between the N TLSs, referred to as the "Dicke state." Under the simplifying assumption of a constant all-with-all interaction I (see Fig. 1), our model reduces to the (isotropic version of the) Lipkin-Meshkov-Glick (LMG) model [9], which originated in the context of nuclear physics but became popular in many other fields [10–13]. We then can use the language of spin states to exploit the resulting approximate permutation symmetry, where the collective Dicke state corresponds to the "large-spin" state.

The energy difference between these many-body states depends on an interaction parameter I and also scales with N. Such interactions between a small number ($N = 2,3$) of qubits have been implemented, e.g., in superconducting circuits [14,15], and it was suggested that these systems could, in principle, be scalable to larger N and realize the LMG model [16]. The question then is the fate of these states in the presence of a noisy environment.

Our model is relevant for the dye-filled microcavity experiments of Klaers *et al.* [17]. Each dye molecule contains both an electronic excitation approximated by a TLS *and* a set of vibrational states (see Fig. 1). In addition, the molecules are coupled to the environment: phonons of the solvent or substrate.

As we calculate, the coupling to the environment allows for transitions between the various collective states (e.g., between the largest spin state and smaller spin states) or, equivalently, to a randomization of the phases in the quantum superposition state. However, although the local decoherence could be so strong [18] as to prevent coherent behavior of a single TLS, it is reasonable to think that since each TLS is coupled to $O(N)$ other molecules, for large enough N decoherence will become the subdominant perturbation compared to the many-body interaction [6]. In this paper we substantiate this idea with explicit calculations of the collective-level decay rates and their consequences for the molecular spectra. Conventionally, molecular spectra contain broadening and satellite vibrational peaks with the associated Franck-Condon effect. We find that when a collective state forms, the emission-line shape has (i) a $1/N$ suppression of the width, (ii) a $1/N$ suppression of vibronic satellites, and (iii) $O(\sqrt{N})$ shifts of the position of the peak. These effects directly imply that transitions observed in the emission are not intra- but rather intermolecular processes.

The essence of the competition between decoherence and interaction can be understood as follows: for a single TLS the effect of decoherence is a fluctuating phase ϕ in the quantum superposition state $|\uparrow\rangle + e^{i\phi}|\downarrow\rangle$, where $|\downarrow\rangle, |\uparrow\rangle$ are the ground and excited states of a single TLS. This phase does not change the energy. However, once multiple TLSs interact, the phase does modify the energy: for example, for $N = 2$ TLSs, one can consider a quantum superposition $|\uparrow\downarrow\rangle + e^{i\phi}|\downarrow\uparrow\rangle$; in this case $e^{i\phi} = +1$ and -1 correspond to triplet and singlet spin states, respectively, which have different interaction energies. For sufficiently large N such energy differences scale as N and can exceed the thermal energy that can be supplied by the environment, and hence, these "large-spin states" become stable against decoherence.

Many-body states with defined total spins can also appear in gases of ultracold spinor atoms, with no coupling to the cavity modes. A mechanism for their stabilization, based on quantum interference, is proposed in Ref. [19].

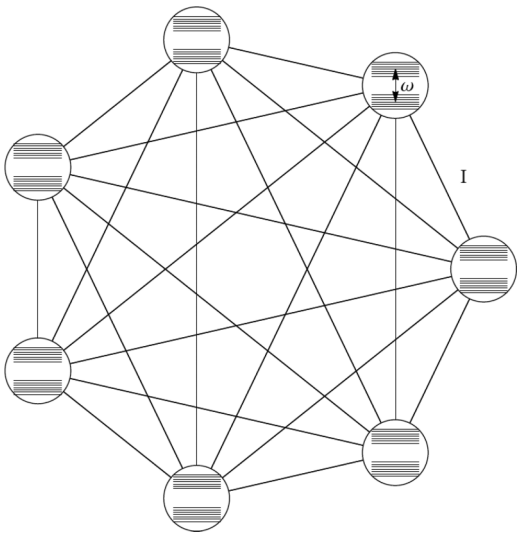

FIG. 1. Maximally connected graph describing N TLSs, with all-to-all interaction I, where each TLS is superimposed on a quasi-continuous set of vibration levels representing local environments and internal vibrational-rotational degrees of freedom of the molecules.

This paper is organized as follows. In Sec. II B we present the model, its collective states, and its relation to the familiar Dicke model. Then, in Sec. III we treat the effect of decoherence due to the environment and compute the decay rate and associated level widths of the collective states. We show that decay to other spin states becomes negligible for a large enough effective interaction parameter (NI) exceeding the thermal energy k_BT. In Sec. IV we discuss the consequences of the interactions in the emission spectrum, which, as we claim in Sec. V, can be observed in experiment. We conclude in Sec. VI.

II. MODEL

A. Cavity-photon-mediated dipole-dipole interaction

We start with the motivation of the all-with-all interaction I in our central model [Eq. (11)]. Consider a two-dimensional optical cavity created between two mirrors of area L^2 and separation d (see Fig. 1 of Ref. [6]). The free-space dispersion relation $\nu_k = c\sqrt{k_x^2+k_y^2+k_z^2}$ now becomes [5]

$$\nu_k = \epsilon_g + \frac{c^2k^2}{2\epsilon_g} = \epsilon_g + \frac{k^2}{2m},\ k=(k_x,k_y), \tag{1}$$

where $\epsilon_g = c\frac{n_z\pi}{d}$ is the cutoff frequency of the cavity ($\hbar=1$) and n_z is a fixed standing wave number. Now we place molecules acting as TLSs in the cavity at positions $(x_i,y_i,z_i) = (r_i,z_i)$, $-L/2 \leqslant x_i,y_i \leqslant L/2, 0 \leqslant z_i \leqslant d$. Our model is

$$H_{cav} = \frac{\omega}{2}\sum_i \sigma_i^z + \sum_k \nu_k a_k^\dagger a_k + \sum_{k,i}(\gamma_{ki}a_k\sigma_i^+ + \text{H.c.}), \tag{2}$$

where $a_k^\dagger$ creates a photon at mode k and

$$\gamma_{k,i} = \gamma e^{ik\cdot r_i}\sin(\pi n_z z_i/d). \tag{3}$$

We define the detuning

$$\Delta = \epsilon_g - \omega \tag{4}$$

and assume it to be sufficiently large and positive such that photons become virtual excitations in the cavity.

Similar to Ref. [20], which studied dipole-dipole interaction induced in a one-dimensional optical cavity (see also Ref. [21]), here we consider the two-dimensional case. Consider an initial state with no photons and one excited TLS at some molecule i_0. The state after time t is

$$|\psi(t)\rangle = \sum_i b_i(t)|\downarrow\downarrow\uparrow_i\downarrow\downarrow\rangle|0\rangle + \sum_k b_k(t)|\downarrow\downarrow\cdots\downarrow\rangle|k\rangle, \tag{5}$$

where $b_i(0)=\delta_{i,i_0}, b_k(0)=0$, and $|k\rangle = a_k^\dagger|0\rangle$. These amplitudes evolve according to the Schrödinger equation

$$\begin{aligned} i\dot{b}_i &= \frac{\omega}{2}(2-N)b_i + \sum_k b_k\gamma_{k,i}, \\ i\dot{b}_k &= \left[\nu_k + \frac{\omega}{2}(-N)\right]b_k + \sum_i \gamma_{k,i}^* b_i. \end{aligned} \tag{6}$$

Using $b_i(t) = b_i(E)e^{i\frac{N\omega}{2}t - iEt}, b_k(t) = b_k(E)e^{i\frac{N\omega}{2}t-iEt}$, solving the Schrödinger equation for $b_k(E)$, and substituting into the equation for $b_i(E)$, we obtain

$$Eb_i = \omega b_i - \sum_j I_{ij}(E)b_j,\ \ I_{ij}(E) = \sum_k \frac{\gamma_{ki}\gamma_{kj}^*}{\nu_k - E}. \tag{7}$$

Using Eq. (3), we obtain, after the angular integration over k,

$$I_{ij}(E) = \sin(\pi n_z z_i/d)\sin(\pi n_z z_j/d)\frac{L^2\gamma^2}{2\pi}\int_0^{1/d} dk k J_0(kr),$$

where $r=|r_i-r_j|$ is the distance between molecules i and j projected to the xy plane. The Bessel function J_0 dictates the relevant k vectors to be $k<1/r$. Since the quadratic dispersion (1) applies only for $k \ll 1/d$, the interaction between two molecules at short distances $r \ll d$ is*not* well described by our approximation. This corresponds to the three-dimensional free-space near-field interaction. For $r \gg d$ we have

$$\begin{aligned} I_{ij}(E) &= \sin(\pi n_z z_i/d)\sin(\pi n_z z_j/d)\frac{L^2\gamma^2 m}{\pi}K_0[r/\ell(E)], \\ \frac{1}{2m\ell^2(E)} &= \Delta - E. \end{aligned} \tag{8}$$

We note a few points: (i) From the asymptotic behavior of the Bessel K function $K_0(x) \to \sqrt{\frac{\pi}{2x}}e^{-x}$ at large x, we see that the interaction decays exponentially over the length $\ell(E)$. (ii) In general one should solve the transcendental Schrödinger equation for E. However, for large detuning $\Delta \gg |E|$ one can ignore the energy dependence of $I_{ij}(E)$ and of $\ell(E)$. Hence,

$$\ell = \frac{1}{\sqrt{2m\Delta}}. \tag{9}$$

(iii) As long as the separation between molecules $\delta \ll d,\ell$ and if $\ell \gg d$, then typical distances between molecules exceed d, and we may disregard near-field interaction. (iv) The prefactors $\sin(\pi n_z z_i/d)\sin(\pi n_z z_j/d)$, which depend on the z positions

of the molecules, will lead to randomness in the interaction I_{ij}. In this paper we will focus on the average effect and ignore these factors.

Under these assumptions, the starting point for this paper is the situation [6] where a number of molecules N whose separation is smaller than ℓ interact with a nearly coordinate-independent two-body interaction $I \sim L^2\gamma^2 m$. Due to the dimensionality mismatch between the molecules, which are spread in the three-dimensional space of the cavity, as opposed to the photons that mediate the interaction, which are two-dimensional due to fixed n_z, the number of molecules in this correlation length becomes [6]

$$N \sim \frac{\ell^2 d}{\delta^3}. \tag{10}$$

This paper deals with effects originating from large values of this number.

B. The model

With the above motivation, we consider the model Hamiltonian $H = H_0 + V$, with $H_0 = H_S + H_v$ and

$$\begin{aligned} H_S &= \frac{\omega}{2}\sum_{i=1}^{N}\sigma_i^z - I\sum_{i,j=1}^{N}\sigma_i^+\sigma_j^-, \\ H_v &= \sum_{i=1}^{N}\sum_{l} E_l v_{l,i}^\dagger v_{l,i}, \\ V &= \sum_{i=1}^{N}\sum_{l}\sigma_i^z(C_l v_{l,i} + \text{H.c.}). \end{aligned} \tag{11}$$

Here H_S describes N TLSs with Pauli operators $\sigma_i^a, a = z,\pm$ $(i = 1,\ldots,N)$. The TLSs are connected via the all-to-all coupling term I, which leads to collective eigenstates described below. The second term, H_v, accounts for the local baths of bosonic modes (vibrations) with energies $\{E_l\}$, created by $v_{l,i}^\dagger$, with mode l at TLS i. The bosonic modes can represent either internal vibrational-rotational molecular degrees of freedom or phonons in the solvent or substrate. We emphasize that there is one independent bath attached to each TLS, and correlations between phonons interacting with different molecules are neglected. Finally, V describes the (linear) coupling between each TLS and its environment, which is an N-spin extension of the usual spin-boson models [2,3].

Due to the permutation symmetry of the model the TLS part of the Hamiltonian H_S can be conveniently written in terms of total spin operators $S^z = \frac{1}{2}\sum_{i=1}^{N}\sigma_i^z, S^\pm = \sum_{i=1}^{N}\sigma_i^\pm$, using the relation $S^+S^- = \mathbf{S}^2 - (S^z)^2 + S^z$, as

$$H_S = \omega S^z - I(\mathbf{S}^2 - S^{z\,2} + S^z). \tag{12}$$

The model (12) when restricted to a specific total spin S, with $\mathbf{S}^2 = S(S+1)$, is known as (a special case of) the LMG model. However, in our system there are many different values of S that N TLSs can form, leading to the spectrum in Fig. 2. As we will discuss below, the environment can cause *transitions* between these states.

The energy of the eigenstates of H_S

$$E_{S,S^z} = \omega S^z + I[S^{z\,2} - S^z - S(S+1)] \tag{13}$$

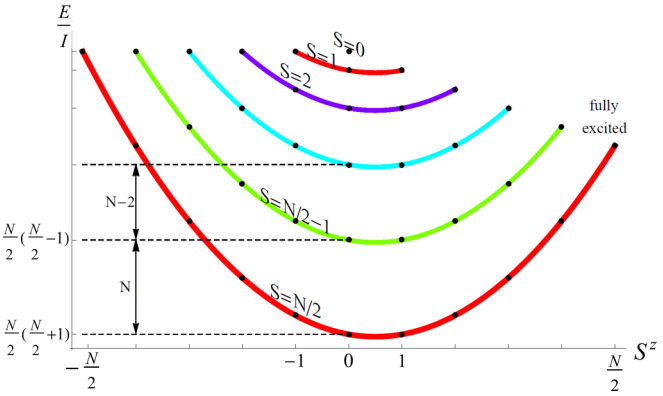

FIG. 2. Energy levels of the LMG model (12) (here $\omega = 0$). Different parabolas correspond to different total spin S. The largest spin state $S = N/2$ is the lowest in energy, with a gap $\delta E = NI$ to the next spin $S = N/2 - 1$ state. For nearly 50% polarization with $|S^z| < N^{1/2}$, we have an energy window IN, in which the large-spin states are well separated (in energy) from all other states.

depends on the total spin S and on the polarization S^z. The maximal total spin formed out of N TLSs, each of which behaves as an elementary spin-$\frac{1}{2}$, is $S_{\max} = N/2$. As can be seen in Fig. 2 this large spin state gains the maximal interaction energy of $-I(N/2)(N/2+1)$ when $I > 0$. The next large spin state, with $S = N/2 - 1$, has a reduced interaction energy gain $-I(N/2-1)(N/2)$ and so on. Thus, typical energy spacings between collective states are given by IN, scaling with the number of TLSs. While in this paper we consider $I > 0$, which is a result of the second-order perturbation theory for $\Delta > 0$ and yields a large-spin ground state, let us remark that in the opposite case ($I < 0$), the ground state corresponds to the *minimal* possible total spin $S = |S^z|$ for given S^z.

There are generically multiple energy-degenerate states with the same values of S and S^z that can be formed out of N TLSs. This number is given by [22]

$$f_S(N) = \frac{N!(2S+1)}{\left(\frac{N}{2}+S+1\right)!\left(\frac{N}{2}-S\right)!}. \tag{14}$$

We label these states by $t = 1,\ldots,f_S(N)$, and thus, a general state is labeled $|\mathcal{S}\rangle = |S,S^z,t\rangle$. There is a single large-spin state $f_{N/2}(N) = 1$ and $N-1$ states with $S = N/2-1$ and so on.

If $I = 0$, the states with different S are energy degenerate and can be transformed to another set of energy-degenerate states, corresponding to defined individual spin and vibrational states of each molecule. However, the energy splitting due to finite I (see Fig. 2) invalidates such a transformation, and the individual states become undefined. A similar effect of spin-independent coordinate-dependent interactions between particles has been noticed already by Heitler [23].

We will see below a protection of the large-spin states against the influence of decoherence.

C. Relation to the Dicke model

Model (12) can be derived from the Dicke model

$$H_D = \sum_k \nu_k a_k^\dagger a_k + \omega S^z + \sum_k(\gamma a_k S^+ + \text{H.c.}), \tag{15}$$

which is just Eq. (2) in the limit where all the molecules under consideration are at the same point. As we now describe, the LMG model (12) is obtained for large enough ϵ_g, where the photons can be "integrated out" and lead to an effective interaction between the N TLSs.

Indeed, the Dicke Hamiltonian commutes with (i) the total number of excitations $N_{\rm ex} = \sum_k a_k^\dagger a_k + \sum_i \frac{\sigma_i^z+1}{2}$ and with (ii) the total spin operator $\mathbf{S}^2 = S(S+1)$. For every value of $(N_{\rm ex}, S)$, as long as $N_{\rm ex} \leqslant N$, there can be $n_{\rm ph} = 0, 1, \ldots, N_{\rm ex}$ photons, with the energy cost $\geqslant n_{\rm ph}\epsilon_g$. When $\epsilon_g > \omega$ and $\epsilon_g - \omega \gg k_B T$, only the zero-photon $n_{\rm ph} = 0$ states survive in the low-energy limit. Then $N_{\rm ex} = S^z + \frac{N}{2}$ ($n_{\rm ph} = 0$). However, one can gain energy from virtual creation and annihilation of photons. The transition amplitude from a state with S^z to $S^z - 1$ via emission of a virtual photon involves the well-known factor

$$S^-|S,S^z\rangle = \sqrt{S(S+1) - S^z(S^z-1)}|S,S^z-1\rangle. \quad (16)$$

Hence, in second-order perturbation theory we obtain a correction to the energy,

$$\delta E = -I[S(S+1) - S^z(S^z-1)] + O(\gamma^4), \quad (17)$$

which is just the LMG model with

$$I = \sum_k \frac{\gamma^2}{\nu_k - \omega}. \quad (18)$$

The emergence of the LMG model as the low-energy limit of the Dicke model is illustrated in Fig. 3.

We mention that the Dicke model displays a phase transition with spontaneously excited photons [24]. Here we will not discuss this superradiant state. The absence of this phase transition is guaranteed (i) at zero temperature for $N\gamma_0^2 < \omega\epsilon_g$, where $\gamma_0^2 = \sum_k \frac{\epsilon_g}{\nu_k}\gamma^2$, and, otherwise, (ii) by $T > T_c$, where T_c is given by $\tanh\frac{\omega}{2k_B T_c} = \frac{\epsilon_g \omega}{\gamma_0^2}$ [24]. However, even in the superradiant phase, there are virtual photons that will mediate the interaction between TLSs.

D. Two-state vibration toy model

Before moving to a study of the effects of decoherence in the next section, we here incorporate effects of *discrete* vibrational modes within a simplified model amenable to exact diagonalization for small systems. In this model we keep only two vibrational states per molecule labeled by $\tau_i^z = \pm 1$, generalizing the Dicke model (15) to

$$H_D' = \omega S^z + \sum_{i=0}^{N}\left(\epsilon\tau_i^z + C\sigma_i^z\tau_i^x\right) + \left(\sum_k \gamma a_k S^+ + \text{H.c.}\right) + \sum_k \nu_k a_k^\dagger a_k. \quad (19)$$

We now use this tractable model to test the fate of the collective levels in the presence of coupling to discrete vibrational modes.

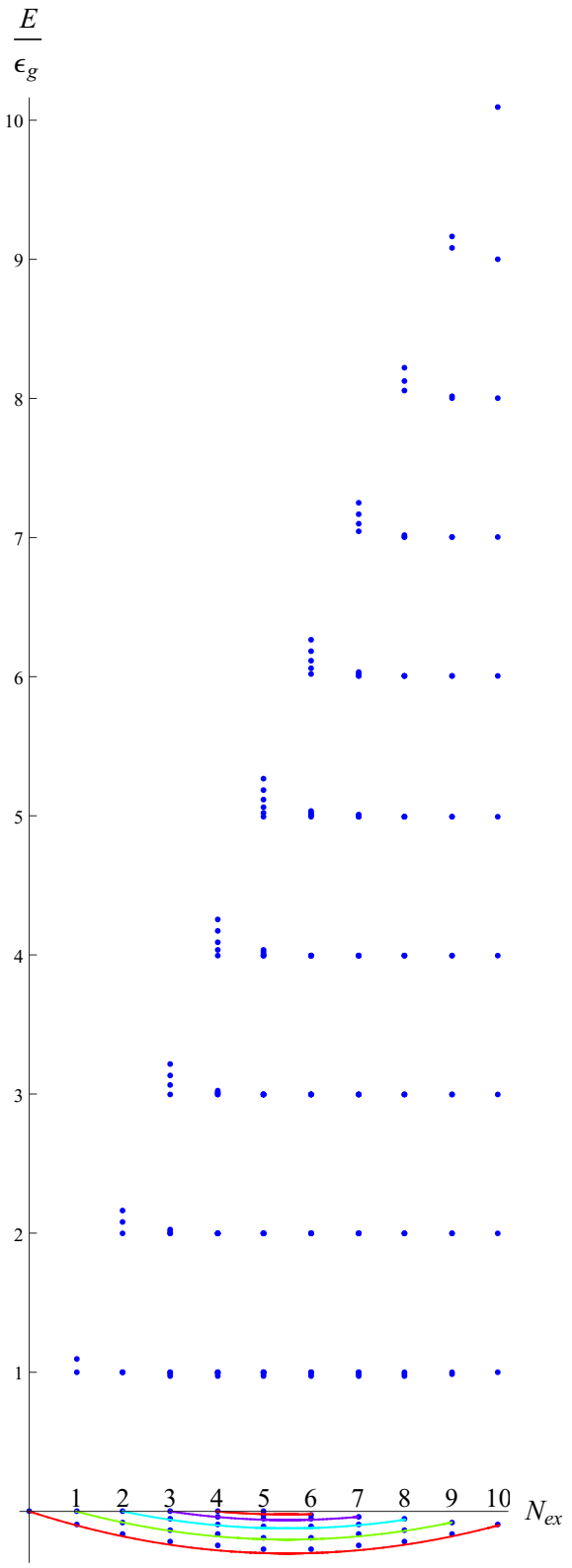

FIG. 3. Full energy spectrum of the single-mode Dicke model (15) obtained by exact diagonalization, with $\epsilon_g = 1, \omega = 0, N = 10$, and $\gamma = 0.2$. One can see that the n-photon states are approximately quantized in units of ϵ_g. The $n = 0$ states are repelled to a negative energy. The fit of the zero-photon states to the LMG model (12) with $I = \frac{\gamma^2}{\epsilon_g}$ is shown by solid parabolic lines (different colors correspond to different values of S as in Fig. 2).

After integrating out the photons, assuming large detuning $\Delta = \min_k \nu_k - \omega \gg \epsilon$,C, we obtain

$$H_{\rm eff} = \omega S^z + \sum_i \left(\epsilon \tau_i^z + C\sigma_i^z \tau_i^x\right) + H_{\rm int},$$
$$H_{\rm int} = -I \sum_{ij} \sigma_j^+ \sigma_i^-, \tag{20}$$

where I is given in Eq. (18). Conventionally, one first diagonalizes the local vibration Hamiltonian $H_\tau(\sigma^z) = \epsilon\tau^z + C\sigma^z\tau^x$ for each state of the electronic TLS $\sigma^z = \pm 1$. Thus, we may define two bases for the vibrational Hilbert space as eigenstates of $H_\tau(\sigma^z)$ for either value of $\sigma^z = \pm 1$:

$$\text{Basis 1: } H_\tau(1)|\pm_\uparrow\rangle = \pm\sqrt{\epsilon^2 + C^2}|\pm_\uparrow\rangle,$$
$$\text{Basis 2: } H_\tau(-1)|\pm_\downarrow\rangle = \pm\sqrt{\epsilon^2 + C^2}|\pm_\downarrow\rangle. \tag{21}$$

Then, while the local part of the Hamiltonian is diagonal, the interaction creates vibrational transitions

$$H_{\rm int} = -I \sum_{i,j} \sigma_j^+ \sigma_i^-$$
$$\times (|+_\uparrow\rangle \ \ |-_\uparrow\rangle)_j \begin{pmatrix} \langle +_\uparrow|+_\downarrow\rangle & \langle +_\uparrow|-_\downarrow\rangle \\ \langle -_\uparrow|+_\downarrow\rangle & \langle -_\uparrow|-_\downarrow\rangle \end{pmatrix} \begin{pmatrix} \langle +_\downarrow| \\ \langle -_\downarrow| \end{pmatrix}_j$$
$$\times (|+_\downarrow\rangle \ \ |-_\downarrow\rangle)_i \begin{pmatrix} \langle +_\downarrow|+_\uparrow\rangle & \langle +_\downarrow|-_\uparrow\rangle \\ \langle -_\downarrow|+_\uparrow\rangle & \langle -_\downarrow|-_\uparrow\rangle \end{pmatrix} \begin{pmatrix} \langle +_\uparrow| \\ \langle -_\uparrow| \end{pmatrix}_i. \tag{22}$$

Explicitly, the matrix elements are

$$\begin{pmatrix} \langle +_\uparrow|+_\downarrow\rangle & \langle +_\uparrow|-_\downarrow\rangle \\ \langle -_\uparrow|+_\downarrow\rangle & \langle -_\uparrow|-_\downarrow\rangle \end{pmatrix} = \begin{pmatrix} \cos(\alpha) & \sin(\alpha) \\ -\sin(\alpha) & -\cos(\alpha) \end{pmatrix}, \tag{23}$$

where $\tan(\alpha) = C/\epsilon$. We see that in the local eigenbasis, the interaction $\sigma_j^+\sigma_i^-$, which flips two TLSs at molecules i, j, also creates transitions in the vibrational states. The squares of the matrix elements (23) are our two-state model version of Franck-Condon factors. This leads to eigenstates of the full system in which vibrations and electronic TLSs are generally entangled.

However, this coupling between TLSs and vibrations can be strongly suppressed in the regime of dominating interactions. Assuming that the interaction I is large enough, we can neglect mixing of states with different S. If we are in the lower-energy large $S = N/2$ spin state, which is permutation symmetric, we can replace the operator σ_i^z in the interaction term $\propto C$ in Eq. (20) by

$$\sigma_i^z \to 2S^z/N \tag{24}$$

(see Sec. IV B). Then for the large-spin state the Hamiltonian becomes independent of the spin states of individual molecules

$$H \to H_S(S, S^z) + \sum_i \left(\epsilon\tau_i^z + \frac{2S^z}{N} C\tau_i^x\right) = H_S(S, S^z)$$
$$+ \sqrt{\epsilon^2 + \left(\frac{2S^z}{N}C\right)^2}$$
$$\times \sum_i [|+^{S^z}(i)\rangle\langle +^{S^z}(i)| - |-^{S^z}(i)\rangle\langle -^{S^z}(i)|]. \tag{25}$$

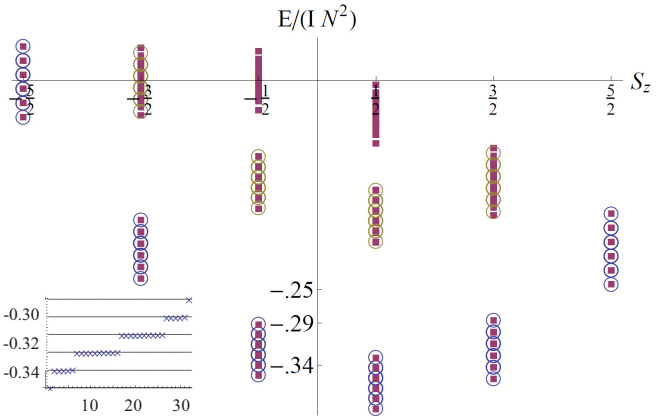

FIG. 4. Spectrum of model (19) for $N = 5, I = 1, \epsilon = C = 0.15$ obtained by exact diagonalization (squares). Each level of the LMG model as in Fig. 2 splits to 2^N vibrational states. Circles are fit to Eq. (25). The inset shows the 32 energy levels corresponding to $S_z = -1/2, S = 5/2$ versus Eq. (25).

Here the vibrational eigenfunctions $|\pm^{S^z}\rangle$ and their eigenenergies depend only on the total many-body spin projection, unlike the eigenstates in Eq. (21), which depend on the individual spins. In the vibrational ground state all the molecules are in the $|-^{S^z}\rangle$ state. The first vibrational excitation of the full system corresponds to exciting one molecule to the state $|+^{S^z}\rangle$.

This separation of the spectrum into the sum of the decoupled TLS part and the vibration part, which depends only on S^z, is confirmed by an exact diagonalization of the model (19), as shown in Fig. 4. We can see that it matches the energy levels of the large-spin $S = N/2$ manifold as well as smaller-spin states. This decoupling is not exact; it relies on the formation of large spin, which is justified for large $IN \gg C$.

We will return to this simplified model in Sec. IV to explicitly demonstrate the suppression of vibrational satellites in the emission spectrum.

III. DECAY RATES OF COLLECTIVE STATES

To study how the many-body states are influenced by coupling to a *continuum* of bath modes, we integrate out the latter and obtain an effective theory of the spin system. We keep referring to these bosonic modes as "vibrations," although their origin can be different, as in general spin-boson models [2,3].

We use the resolvent formulation whose poles give the spectrum of the system. Expanding the resolvent of the full system $R(z) = (z - H)^{-1}$ in powers of V and tracing over the vibrations, one obtains (for details see, for example, Ref. [25])

$$R(z) = \frac{1}{z - H_S - \Sigma(z)}, \tag{26}$$

with the self-energy

$$\Sigma(z) = \sum_{\{v\}} n_B(E_{\{v\}}) V (z + E_{\{v\}} - H_0)^{-1} V. \tag{27}$$

Here $n_B(E) \propto e^{-E/(k_B T)}$ is the normalized Boltzmann distribution. The imaginary part of $\Sigma(z)$ gives the Fermi's-golden-rule

transition rate between different spin states mediated by exchange of vibration quanta. We denote

$$\Gamma_{\mathcal{S}} = -\mathrm{Im}\Sigma(z = E_{S,S^z} + i\delta) \tag{28}$$

as the inverse half-life time of the spin state $|\mathcal{S}\rangle$. As discussed in more detail in Appendix A, the selection rules, mediated by V, allow exclusively for $S \to S, S \pm 1$ transitions. They provide three terms in the decay rate of the collective state,

$$\Gamma_{S,S^z} = \frac{2\pi}{2S+1}\sum_{S'}\left\{\delta_{S',S}\left[(N/2+S+1)\frac{S^{z2}}{S} + (N/2-S)\frac{S^{z2}}{S+1}\right]\mathcal{A}(0)\right.$$
$$\left. + \delta_{S',S+1}(N/2-S)\frac{(S+1)^2 - S^{z2}}{S+1}\mathcal{A}(E_{S+1,S^z} - E_{S,S^z}) + \delta_{S',S-1}(N/2+S+1)\frac{S^2 - S^{z2}}{S}\mathcal{A}(E_{S-1,S^z} - E_{S,S^z})\right\}. \tag{29}$$

In the case of $N = 1, S = S' = S^z = 1/2$, this equation gives the level width of a single molecule [26],

$$\Gamma_{1/2,1/2} = \pi\mathcal{A}(0) = \frac{1}{2T_2}. \tag{30}$$

Then the spectral function $\mathcal{A}(0)$ is related to the single-molecule relaxation time T_2.

Equation (29) is the main result of this section. We now discuss its content. The terms $\propto \delta_{S',S\pm1}$ correspond to transitions $S \to S' \neq S$. Starting from a large-spin state $S \sim N/2$ and for a nearly unpolarized state $|S^z| \ll S$, we see from the overall coefficients that transitions $S \to S+1$ are suppressed by a factor $(\frac{N}{2} - S)$ (which exactly vanishes for $S = N/2$), while transitions $S \to S-1$ have an increased rate $\propto N$, which is the phase space corresponding to the number of possible final states with smaller spin, Eq. (14). However, transitions from the large-spin state require a finite energy to be extracted from the vibrational baths. The thermal energy $k_B T$ will be exceeded by the required energy difference $E_{S-1,S^z} - E_{S,S^z} = IN$ for large enough N. Thus, $\mathcal{A}(E) \propto n_B(E) \to 0$ for

$$IN \gg k_B T. \tag{31}$$

Then the large-spin state becomes *stable*.

The most prominent regime to study this large-spin state is near the unpolarized state where $(S^z)^2 \leqslant N$. As can be seen in Fig. 2, this corresponds to the lowest-energy window of size $\delta E = (IN)$, which includes only the large $S = N/2$ manifold, with $\sim \sqrt{N}$ states.

In this large interaction regime only the terms $\propto \mathcal{A}(0)$ in Eq. (29), leaving S fixed, contribute. These terms, however, are of order $\frac{(S^z)^2}{S}$, that is, are suppressed for large N. Thus,

$$\Gamma_{S,S^z} \cong \frac{1}{NT_2} \quad [S = N/2, S^z = O(1)]. \tag{32}$$

Thus, the large-spin state enjoys a $1/N$ reduction of the dephasing rate.

We note that the result (29) is not valid for $I = 0$ since it assumes initial and final *collective* states, while for $I = 0$ processes of decoherence happen within a single molecule or in its near vicinity. Self-consistently, to ensure the stabilization of collective states we demand $IN \gg \Gamma_{S,S^z}$.

The real part of the self-energy $\Sigma = \Sigma' + i\Sigma''$ provides information on energy shifts of the spin states due to their coupling to the vibrations. In Appendix B we estimate these corrections and find that they are subdominant; namely, they are of order $O(1)$, compared to the $O(N)$ energy difference between collective states.

IV. MOLECULAR EMISSION SPECTRUM

A. Spectral line widths and shifts

We now discuss physical signatures of the collective states in the emission spectrum. For comparison, for a single TLS the emission spectrum has a Lorentzian line shape with $W(E) \propto [E - (\omega + \Delta\omega) + (1/T_2)^2]^{-1}$, where $\Delta\omega$ is an energy shift and T_2 results from decoherence. Both the position and width of the peak are modified in a system of N TLSs (see, for example, related studies involving plasmons or polaritons [27,28]). Here we will identify the role of interactions and pinpoint how these effects in the emission spectrum scale with N.

For simplicity consider an identical coupling of the N TLSs to classical light,

$$\delta H = \Omega\sum_i \sigma_i^- e^{iEt} + \mathrm{H.c.} = \Omega S^- e^{iEt} + \mathrm{H.c.} \tag{33}$$

Notice that we are implicitly distinguishing the emitted photons from the cavity photons mediating the interaction. The latter are emitted and absorbed multiple times, which is assisted by the cavity. On the contrary, the emitted photons contributing to the emission spectrum $W(E)$ propagate in free space and yet have a finite coupling to the TLSs inside the cavity.

Emission occurs via transitions $S^z \to S^z - 1$. Consider the system in an initial state $|i\rangle = |S, S^z, t\rangle$. As shown in Appendix C, the transition rate to the final state $|f\rangle = |S, S^z - 1, t'\rangle$ is proportional to

$$W(E) \propto \Omega^2 |\langle f|S^-|i\rangle|^2 \times \frac{\Gamma_i + \Gamma_f}{[\omega + 2I(S^z - 1) + \Sigma_i' - \Sigma_f' - E]^2 + (\Gamma_i + \Gamma_f)^2}. \tag{34}$$

The level widths $\Gamma_{i,j}$ and the level shifts $\Sigma'_{i,f}$ were introduced in the previous section; it is assumed that the width is dominated by the vibrational modes rather than by the coupling Ω to the emitted light, namely, $\Gamma_{i,f} \gg \Omega$. A few effects apparent in Eq. (34) should be noted.

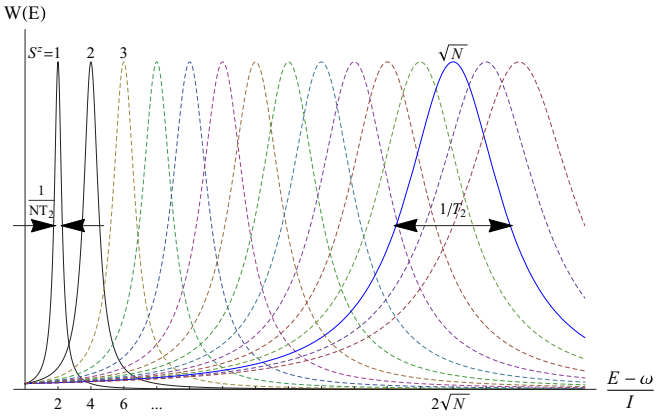

FIG. 5. Schematic depiction of the emission spectrum of N interacting TLSs. Different peaks correspond to different initial values of S^z with the peak positions given in Eq. (36) up to $O(1)$ additional level shifts. In the large-S regime the level width increases with S^z as $\Gamma \sim [(S^z)^2/S] \times 1/T_2$, reaching values of order $1/T_2$ for $S^z \sim N^{1/2}$ and values of order $1/(NT_2)$ for $S^z \ll S$.

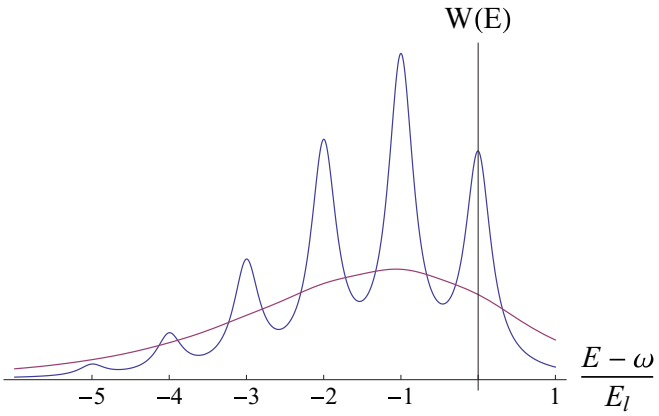

FIG. 6. Schematic depiction of the emission spectrum of one molecule, including (i) vibrational satellites (for one mode l) according to the Franck-Condon factor (40) and (ii) additional broadening $1/T_2 = 0.5E_l$ (brown) and $0.1E_l$ (blue). Here $C_l/E_l = 0.6$.

(i) The Dicke factor [see Eq. (16)] strongly depends on S^z:

$$|\langle f|S^-|i\rangle|^2 \propto \begin{cases} N, & S^z \sim N/2, \\ N^2, & S^z = O(1). \end{cases} \tag{35}$$

This Dicke enhancement factor is *independent* of the interactions between the TLSs.

(ii) The energy of the transition $(S,S^z) \to (S,S^z-1)$,

$$\omega_{S^z} = E_{S,S^z} - E_{S,S^z-1} = \omega + 2I(S^z-1), \tag{36}$$

is strongly shifted by the interactions depending on the polarization state S^z. Focusing on the lowest-energy window $\delta E = NI$ in Fig. 2, with $|S^z| < O(\sqrt{N})$, this shift is of order $\sqrt{N}$. It overcomes the level shifts $\Sigma'_{i,f}$ of order unity.

(iii) Following Eq. (32), the width of the emission line $\Gamma_i + \Gamma_f$ is strongly suppressed. Specifically, the peak width is N times sharper than the single-molecule linewidth $1/T_2$ for $S^z = O(1)$ and becomes of order $1/T_2$ for $S^z \sim \sqrt{N}$. This is depicted schematically in Fig. 5.

Along the cascade of decay due to emission, $S^z \to S^z - 1 \to S^z - 2$, which can be analyzed, e.g., by solving rate equations, the system is in a probabilistic superposition of collective states with different S^z. Then the emission spectrum also contains a superposition of peaks whose positions and widths are shown in Fig. 5. They will become well isolated if $IN \gg \frac{1}{T_2}$. The relative peak heights in Fig. 5 along this cascade were not calculated here.

B. Vibrational structure of the emission spectra

1. *Suppression of satellites for permutation-symmetric spin states*

Transitions between discrete vibrational levels typically lead to additional peaks in the emission spectrum, here referred to as Franck-Condon "satellites." We have ignored these satellites above. However, we now demonstrate that this was done with a good reason: in the large-interaction limit these satellites are suppressed as $1/N$.

The emission spectrum

$$W(E) = \sum_{E_{fi}} a(E_{fi})\delta(E + E_{fi}) \tag{37}$$

contains several peaks. The peak intensities $a(E_{fi})$ are determined by the matrix elements of the interaction (33) with the classical field as

$$a(E_f - E_i) = 2\pi\Omega^2 |\langle \Psi_f|S^-|\Psi_i\rangle|^2. \tag{38}$$

Here $|\Psi_i\rangle$ and $|\Psi_f\rangle$ are eigenstates of the Hamiltonian (11), corresponding to the total spin projections S^z and S^z-1, respectively, and E_i and E_f are their eigenenergies.

For one molecule, vibrational transitions occur due to the linear coupling C_l in Eq. (11), which we write for clarity for one mode of energy E_l as

$$\begin{aligned} H_{\mathrm{vib},\uparrow} &= E_l v^\dagger_{l,i} v_{l,i} + (C_l v_{l,i} + \mathrm{H.c.}), \\ H_{\mathrm{vib},\downarrow} &= H_{\mathrm{vib},\uparrow} - 2C_l(v_{l,i} + \mathrm{H.c.}). \end{aligned} \tag{39}$$

The transition from the vibrational ground state $|0_\uparrow\rangle$ to a final excited vibrational state $|n_\downarrow\rangle$ $(n \geqslant 0)$ corresponds to the peak with the intensity $a(\omega - nE_l) = 2\pi\Omega^2 F_n(C)$, where the Franck-Condon factor is explicitly given by

$$F_n(C) = |\langle n_\downarrow|0_\uparrow\rangle|^2 = \frac{1}{n!}\left(\frac{2C_l}{E_l}\right)^{2n} \exp\left(-\frac{4C_l^2}{E_l^2}\right). \tag{40}$$

The resulting emission lines are shown in Fig. 6.

For many molecules the Hamiltonian (11) commutes with S^z, and all its terms, except for V, commute with S. In the limit of large IN, the large energy gaps between states with different S (see Fig. 2) allow us to neglect their coupling and consider the projection of the Hamiltonian (11) to the states $|S,S^z,t\rangle$,

$$\begin{aligned} H_{\mathrm{vib},S,S^z} = &\sum_t |S,S^z,t\rangle\langle S,S^z,t|(H_v + V) \\ &\times \sum_{t'} |S,S^z,t'\rangle\langle S,S^z,t'| \end{aligned} \tag{41}$$

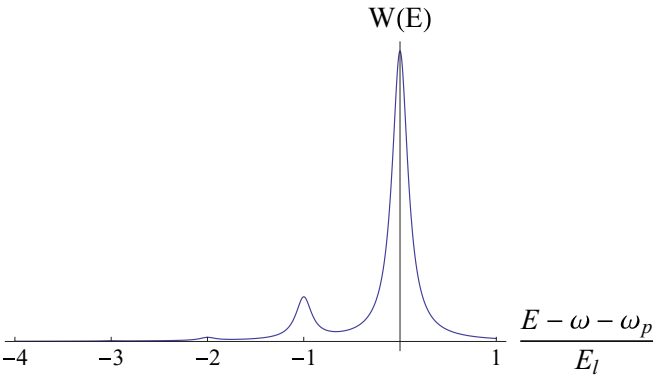

FIG. 7. Schematic depiction of the emission spectrum as in Fig. 6 but for $N = 10$ molecules. Here $1/T_2 = 0.5E_l$, and ω_p is an additional polaronic shift.

(the contribution of H_S is omitted here as it can lead to only an energy shift). Suppose now that N TLSs form a large-spin $S = N/2$ state. As this state $|N/2, S^z\rangle$ is symmetric with respect to permutations of the molecular spins,

$$\langle N/2, S^z|\sigma_i^z|N/2, S^z\rangle = \frac{1}{N}\langle N/2, S^z|\sum_i \sigma_i^z|N/2, S^z\rangle. \quad (42)$$

Then the vibration Hamiltonian becomes

$$H_{\mathrm{vib},N/2,S^z} \to \sum_i E_l v_{l,i}^\dagger v_{l,i} + \frac{2S^z}{N}(C_l v_{l,i} + \mathrm{H.c.}). \quad (43)$$

One can immediately see that the shift of the vibrational potential in the process $S^z \to S^z - 1$ is reduced by a factor $1/N$,

$$H_{\mathrm{vib},N/2,S^z-1} = H_{\mathrm{vib},N/2,S^z} - \frac{2C_l}{N}(v_{l,i} + \mathrm{H.c.}). \quad (44)$$

This leads to dramatic effects in the emission spectrum. The main peak, corresponding to ground vibrational modes of all molecules in the initial and final states, has an intensity

$$a(\omega_{S^z}) = 2\pi\Omega^2\left(\frac{N}{2}+S^z\right)\left(\frac{N}{2}-S^z+1\right)[F_0(C/N)]^N. \quad (45)$$

The first satellite corresponds to a final state with an $n = 1$ excitation in one of the N molecules with intensity

$$a(\omega_{S^z} - E_l) = 2\pi\Omega^2\left(\frac{N}{2}+S^z\right)\left(\frac{N}{2}-S^z+1\right) \times N[F_0(C/N)]^{N-1}F_1(C/N). \quad (46)$$

Similarly, the second and higher satellites can be obtained. The ratio of the first satellite intensity to that of the main peak is given by

$$\frac{NF_1(C/N)}{F_0(C/N)} = \left(\frac{2C_l}{E_l}\right)^2\frac{1}{N}. \quad (47)$$

Hence, we observe a $1/N$ reduction of the satellites. The emission lines based on this analysis are shown in Fig. 7.

In order to characterize the cumulative effect of the satellite suppression, let us introduce the total line intensity

$$a = \int W(E)dE = \sum_f a(E_f - E_i). \quad (48)$$

The summation over f can be expanded over the complete set of states $|\Psi_f\rangle$ since the matrix elements vanish for noncoupled states. Then

$$a = 2\pi\Omega^2|\langle\Psi_i|S^+S^-|\Psi_i\rangle|^2 = 2\pi\Omega^2\left(\frac{N}{2}+S^z\right)\left(\frac{N}{2}-S^z+1\right), \quad (49)$$

and the ratio of the main peak intensity to the total one, given by

$$\frac{a(\omega_{S^z})}{a} = [F_0(C/N)]^N = \exp\left(-\frac{4C_l^2}{NE_l^2}\right), \quad (50)$$

tends to unity at large N. Below we will confirm this effect in the two-state vibration model.

2. *Calculation for the two-state vibration model*

To demonstrate explicitly the picture described above for the satellite suppression, we consider the simplified model of discrete vibrational modes in Sec. II D. The emission lines correspond to transitions between many-body levels (see Fig. 4), where S^z changes by 1. Consider starting from the initial state $|\Psi_i\rangle$, which is the vibrational and electronic ground state with given S^z. For one molecule the electronic transition from $S^z = 1/2$ to $S^z = -1/2$ (or $|\uparrow\rangle \to |\downarrow\rangle$) is associated with two emission peaks with intensities $a(\omega)$ and $a(\omega - 2\sqrt{C^2+\epsilon^2})$. The first peak corresponds to a transition from the vibrational ground state $|-_\uparrow\rangle$ [see Eq. (21)] to the new ground state $|-_\downarrow\rangle$, with matrix element $a_0 = \cos^2(\alpha)$ [see Eq. (23)]. The satellite peak corresponds to a transition to the excited vibrational state $|+_\downarrow\rangle$, with matrix element $a_1 = \sin^2(\alpha)$. Thus, the ratio of the satellite to the main peak intensity is given by $\tan^2(\alpha) = C^2/\epsilon^2$. We now explore how this ratio evolves for a few interacting molecules.

As described in Sec. II D, when I is large enough that we are in the lowest-energy large $S = N/2$ spin state which is symmetric, we can replace the operator σ_i^z in the interaction term $\propto C$ in Eq. (20) by $\sigma_i^z \to 2S^z/N$. The initial and final Hamiltonians of the vibrations are given by $H_\tau(\sigma^z)$ with $\sigma^z = 2S^z/N$ and $\sigma^z = 2(S^z-1)/N$, respectively. We start in the ground state of the configuration with the initial S^z whose energy is $-N\sqrt{\epsilon^2 + (2\frac{S^z}{N}C)^2}$ (all N molecules in the vibrational ground state $|-^{S^z}\rangle$). The main peak is obtained by going to the ground state of the new Hamiltonian with $S^z - 1$ in all the molecules (all N molecules in the new vibrational ground state $|-^{S^z-1}\rangle$), with energy $-N\sqrt{\epsilon^2 + (2\frac{S^z-1}{N}C)^2}$. Thus, the main emission peak occurs at the energy

$$E_{\mathrm{main}} = H_{\mathrm{int}}(S, S^z) - H_{\mathrm{int}}(S, S^z - 1) + \delta E, \quad (51)$$

where we have separated the vibrational contribution

$$\delta E = -N\sqrt{\epsilon^2 + \left(2\frac{S^z}{N}C\right)^2} + N\sqrt{\epsilon^2 + \left(2\frac{(S^z-1)}{N}C\right)^2}.$$

The nth satellite corresponds to flipping n molecules to their vibrational excited state $|+^{S^z-1}\rangle$ and corresponds to the

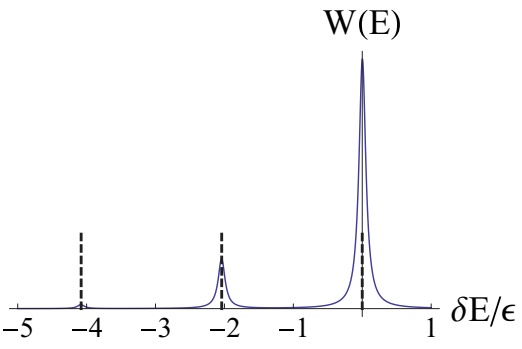

FIG. 8. Emission spectrum for the model (19) with $N = 5, \epsilon = C = 0.01, I = 1$. We start in the $S^z = 1/2$ ground state (belonging to the total spin-5/2 "parabola" in Fig. 4).

emission line

$$\delta E_n = -N\sqrt{\epsilon^2 + \left(2\frac{S^z}{N}C\right)^2} + (N-2n)\sqrt{\epsilon^2 + \left(2\frac{S^z-1}{N}C\right)^2}.$$

This set of satellites and the main peak ($n = 0$) is plotted as dashed lines in Fig. 8 and perfectly agrees with the position of the peaks obtained by computing Fermi's golden rule (37) using the numerically obtained eigenstates for a small ($N = 5$) system with large interaction I.

In addition, the heights of the satellites are strongly suppressed. The height ratio of the strongest satellite to the main peak is

$$N\tan^2\frac{\alpha_{S^z} - \alpha_{S^z-1}}{2},\ \alpha_{S^z} = \arctan\frac{2S^zC}{N\epsilon}. \quad (52)$$

The factor of N counts possible choices of the molecule, in which the excitation $|+^{S^z-1}\rangle$ is located in the final state, and the remaining function is the ratio of matrix elements $\frac{|\langle +^{S^z-1}|-^{S^z}\rangle|^2}{|\langle -^{S^z-1}|-^{S^z}\rangle|^2} = \tan^2\frac{\alpha_{S^z}-\alpha_{S^z-1}}{2}$. The ratio (52) perfectly agrees with the numerical results. Similarly, higher satellite peaks are suppressed by a higher power of this same small factor.

For $S^z = N/2$ and large N this ratio tends to $\frac{1}{N}\frac{(C/\epsilon)^2}{[1+(C/\epsilon)^2]^2}$. For $S^z/N \ll 1$ this ratio becomes $\frac{1}{N}\frac{C^2}{\epsilon^2}$. In either regime we obtain the $1/N$ suppression of the satellites.

To conclude, we have shown a $1/N$ suppression of the vibrational satellites, which is a crucial effect of the collective interacting set of TLSs.

V. OBSERVABILITY

We now discuss the observability of this collective effect in a microcavity filled with dye molecules, referring to the experimental parameters of Klaers *et al.* [17]. The emission line of a single molecule has a typical frequency in the visible range $\omega \sim 500$ THz and a width of the order of 50 THz. This width corresponds to many vibrational satellites broadened by $1/T_2$. The system is at room temperature $k_BT \sim 10$ THz.

Following Ref. [6], the interaction I in our model can be estimated using the typical emission time from a single TLS in the cavity $\tau \sim 3$ ns. This rate is related via Fermi's golden rule to the product of the coupling constant γ^2 and the density of states $\frac{m}{2\pi}$,

$$\frac{1}{\tau} = L^2\gamma^2 m \sim 1\ \text{GHz}. \quad (53)$$

Using Eq. (8), we see that the interaction is determined by the same parameters,

$$I \sim \frac{1}{\tau} \sim 1\ \text{GHz}. \quad (54)$$

This can be negligible compared to the decoherence, which is restricted by the width and can have a value up to $1/T_2 \sim 50$ THz. However, could coherence be restored due to large N? Using Eqs. (10) and (9), we obtain

$$N \sim \left(\frac{c}{\epsilon_g}\right)^3\frac{1}{\delta^3}\frac{1}{(\Delta/\epsilon_g)} \sim \left(\frac{d}{\delta}\right)^3\frac{\epsilon_g}{\Delta}. \quad (55)$$

Since the separation between the mirrors $d = 1.5\ \mu$m exceeds the separation between molecules $\delta \sim 10$ nm by two orders of magnitude and since the detuning is naturally much smaller than the cavity frequency $\epsilon_g = c\frac{n_z\pi}{d} \approx 10^{15}$ Hz (the standing wave number is $n_z = 7$), we expect large values of N, which are required to satisfy the condition $IN \gg 1/T_2, k_BT$. For example, for a detuning of $\Delta/\epsilon_g = 0.05$ (5% detuning), we obtain $N \sim 3000$. As the decoherence rate is quite large in this experiment, giving an estimate for the decoherence to interaction ratio $(1/T_2)/I \sim 10^4$, we see that further experimental fine-tuning is required to reach the conditions of the present proposal, as we discuss in more detail subsequently.

While the experiment [17] concentrated on Bose-Einstein condensation of photons at room temperature, the present scenario requires (i) large detuning $\Delta > 0$ so as to push the cavity mode to high frequencies compared to the TLS transition, (ii) lower temperature, leading to reduced $1/T_2$, and (iii) a high polarization state (nearly half of the TLSs in the excited state). In addition, our estimate of N should be taken with a grain of salt, as it was obtained using crude assumptions of constant interaction strength I_{ij}, ignoring near-field effects as well as fluctuations in its sign due the $\sin(z_i n_z\pi/d)$ factors in Eq. (3) and the $n_z > 1$ condition in the experiment.

VI. CONCLUSIONS

We studied a competition between local decoherence and all-with-all interaction between N TLSs. The physical situation considered here, where each TLS contains a separate bath of oscillators, may be realized in an ensemble of dye molecules in an optical microcavity. The many-body physics studied here corresponds to a rather unexplored regime, with nearly equal population of excited and deexcited TLSs.

The effect of interaction between TLSs is a formation of a many-body states, which results, e.g., in a strong shift of the emission line, level narrowing by $1/N$, and a $1/N$ suppression of vibrational satellites. Thus, these collective states remain coherent despite the noise on the individual molecules.

Interactions, mediated by two-dimensional cavity modes, also allow us to control many-body states of two-level atoms, where the obstructing effects of molecular vibrations are absent.

We considered an ideal system with equal interaction between all TLSs, ignoring effects of disorder. A more generic model for the interaction Hamiltonian is $-\sum_{i,j} I_{ij}\sigma_i^+\sigma_j^-$, with $I_{ij} \propto \gamma_i\gamma_j$ with random $\{\gamma_i\}$, e.g., due to the random $\{z_i\}$ locations. We speculate that the emergence of large-spin states separated by a large energy $\propto (IN)$ from all other states is a robust effect that survives in the presence of disorder. Proving this assertion is left for a future study.

Note added in proof. Recently, two related works have appeared on the ArXiv [29,30]. Following communications with J. Keeling, we found that our work may be related to the experiment in Ref. [31], observing coherent coupling of molecular resonators with a microcavity mode, and subsequent theoretical analysis [32–34].

ACKNOWLEDGMENTS

We thank I. Carusotto, E. Dalla Torre, M. Goldstein, A. Nitzan, and A. Russomanno for discussions and acknowledge funding from Israel Science Foundation Grant No. 1243/13 (E.S.) and Grant No. 1309/11 (V.F.) and from Marie Curie CIG Grant No. 618188 (E.S.). V.F. is grateful to PCS IBS, Daejeon, Korea, for hospitality.

APPENDIX A: CALCULATION OF THE LEVEL WIDTH

The Hamiltonian H_0 contains H_S [see Eq. (11)], which is independent of the molecular vibrational and translational coordinates, and H_v, which is independent of the electronic degrees of freedom, treated here as spins. Each of the parts is permutation invariant. Therefore, the total many-body wave function is represented as (see [22,35])

$$\tilde{\Psi}^{(S)}_{r\{v\}S_z} = f_S^{-1/2}\sum_t \tilde{\Phi}^{(S)}_{tr\{v\}}|S,S^z,t\rangle. \tag{A1}$$

Here the spin $|S,S^z,t\rangle$ and spatial $\tilde{\Phi}^{(S)}_{tr\{v\}}$ wave functions form bases of irreducible representations of the symmetric group associated with the Young diagram $\lambda = [N/2+S, N/2-S]$. These representations have dimensions $f_S(N)$ [see Eq. (14)], and the labels of the basic functions t are standard Young tableaux of the shape λ. For bosons, the representation of the spatial wave functions is associated with the same Young diagram λ, while for fermions it is associated with the conjugate diagram $[2^{N-S/2},1^S]$. This provides the correct bosonic or fermionic permutation symmetry of the total wave function. The Young tableaux r label different representations, associated with the same Young diagram.

In the wave function (A1) the spatial wave functions are represented as symmetrized wave functions of noninteracting dye molecules in the vibrational-translational states $|v_i\rangle$ with energies E_{v_i}. Equation (A1) neglects two-body coordinate-dependent interactions between the molecules. In a thermal system, multiple occupation of a translational state has negligible probability. Thus, all v_i are different, although several molecules can be in the equal vibrational states.

States with different total spins can be mixed by interactions which depend on both spins and coordinates. In the present case, the relevant interaction has the form

$$V = \sum_i \frac{1}{2}\sigma_i^z U(i). \tag{A2}$$

Here spin-independent $U(i)$ can describe both interactions with internal degrees of freedom, e.g., the linear coupling of Eq. (11), and arbitrary interactions with the environment dependent on the internal and translational coordinates of the molecule.

The lifetime of the many-body states is determined by the imaginary part (28) of the self-energy, calculated with Fermi's golden rule,

$$\mathrm{Im}\Sigma(z = E_{SS^z} + i\delta) = -\pi \sum_{\{v\},\{v'\},r',S'} \left|\left\langle \tilde{\Psi}^{(S')}_{r'\{v'\}S_z}\middle|V\middle|\tilde{\Psi}^{(S)}_{r\{v\}S_z}\right\rangle\right|^2 \times n_B(E_{\{v\}})\delta\left[E_{S',S^z} - E_{S,S^z} + \sum_i (E_{v'_i} - E_{v_i})\right]. \tag{A3}$$

The S^z dependence of the matrix elements can be extracted by using the Wigner-Eckart theorem [see Eq. (23) in [35]]. Then the imaginary part (A3), averaged over r, can be calculated with the sum rules [see Eq. (37) in [35]], leading to

$$\begin{aligned}\Gamma_{S,S^z} &= \frac{1}{f_S(N)}\sum_r \Gamma_{\mathcal{S}} \\ &= \pi\sum_{S'}\Big\{\delta_{S',S}Y^{(S,1)}[\hat{U}_0,\hat{U}_0] + \delta_{S',S+1}Y^{(S+1,1)}[\hat{U}_{-1},\hat{U}_{-1}] \\ &\quad + \delta_{S',S-1}Y^{(S,1)}[\hat{U}_{-1},\hat{U}_{-1}]\frac{f_{S-1}(N)}{f_S(N)}\Big\} \\ &\quad \times \left(X^{(S,S',1)}_{S_z0}\right)^2 \sum_{\{v\},\{v'\}} \frac{1}{N}\sum_i |\langle v'_i|U|v_i\rangle|^2 \prod_{i'\neq i}\delta_{v'_{i'},v_{i'}} \\ &\quad \times n_B(E_{\{v\}})\delta\left[E_{S',S^z} - E_{S,S^z} + \sum_i \left(E_{v'_i} - E_{v_i}\right)\right].\end{aligned} \tag{A4}$$

The width contains three terms, corresponding to $S' = S, S\pm 1$, in agreement with the selection rules [36] for the case of one-body interactions. Substituting the factors X and Y [see Eq. (23) and Table I in [35]] and introducing the spectral function

$$\mathcal{A}(E) = \sum_{v,v'} n_B(E_v)|\langle v'|U|v\rangle|^2\delta(E + E_{v'} - E_v), \tag{A5}$$

we get Eq. (29).

APPENDIX B: LEVEL CORRECTIONS

The real part Σ' of the self-energy $\Sigma = \Sigma' + i\Sigma''$ provides information on shifts of energy levels of the spin states due to their coupling to the vibrations. We now demonstrate that these level shifts do not destroy the $O(IN)$ energy separation of the large-spin state from the remaining levels.

The summation over $\{v\},\{v'\},r'$ and averaging over r are done in the same way as for the imaginary part in Appendix A. Then we get Eq. (29), where the spectral function (A5) is replaced by

$$\sum_{v,v'} n_B(E_v)\frac{|\langle v'|U|v\rangle|^2}{E_{S',S^z} - E_{S,S^z} + E_{v'} - E_v}. \tag{B1}$$

(1) *Diagonal virtual transitions* $S' = S$. In this case the denominator in Eq. (B1) is the vibration energy difference and

is independent of the spin state. The factor from Eq. (29) gives a correction to all energy levels

$$\delta E \propto \left(\frac{N}{2}+1\right)\frac{(S^z)^2}{S(S+1)}. \tag{B2}$$

This is negligible for unpolarized states $S^z \ll S$ by a factor of $1/N$.

(2) *Off-diagonal virtual transitions* $S' = S \pm 1$. In this case the energy denominator is dominated by $E_{S\pm1,S^z} - E_{S,S^z} \sim IS$, leading to

$$\delta E \propto \left(\frac{N}{2}+S+1\right)\frac{S^2-S^{z2}}{(2S+1)S^2} - (N/2-S)\frac{(S+1)^2-S^{z2}}{(2S+1)S(S+1)}. \tag{B3}$$

For the large-S states the first term dominates, and this correction is of $O(1)$, much smaller than the energy difference between different S states IS. Furthermore, the dependence of this correction on S^z is only of order $(S^z/S)^2$, again strongly suppressed for unpolarized states.

Thus, the large-spin state remains well separated from the smaller spin states: its separation from the next levels is of $O(N)$, while the level corrections are of $O(1)$.

APPENDIX C: EMISSION RATE

We compute the transition rate between initial (i) and final (f) states, where $S^{z(i)} = S^{z(f)} + 1$. It is related to the matrix element (i,f) of the evolution operator as $\Gamma_{i\to f} = \frac{d}{dt}|U_{fi}(t)|^2$. The transition amplitude occurs due to the perturbation $\delta H = \Omega e^{iEt}S^- + \text{H.c.}$, corresponding to coupling with the emitted electromagnetic radiation.

Denoting the free evolution operator of the decoupled spin system by $\mathcal{U}_0$, the rate of the transition in the absence of vibrations can be written as

$$\begin{aligned}\frac{d}{dt}|U_{fi}(t)|^2 &= \frac{d}{dt}\left[\langle f|\int_0^t dt'\mathcal{U}_0(t,t')V(t')\mathcal{U}_0(t',0)|i\rangle\langle i|\int_0^t dt''\mathcal{U}_0(0,t'')V(t'')\mathcal{U}_0(t'',t)|f\rangle\right]\\ &= \langle f|\int_0^t dt'\mathcal{U}_0(t,t')V(t')\mathcal{U}_0(t',0)|i\rangle\langle i|\mathcal{U}_0(0,t)V(t)\mathcal{U}_0(t,t)|f\rangle + \text{c.c.}\\ &= \Omega^2|\langle f|S^-|i\rangle|^2 e^{-iEt}\int_0^t dt'\langle f|\mathcal{U}_0(t,t')|f\rangle e^{iEt'}\langle i|\mathcal{U}_0(t',t)|i\rangle + \text{c.c.}\end{aligned} \tag{C1}$$

The free evolution operator is related to the free resolvent

$$\mathcal{U}_0(t,0) = \frac{1}{2\pi i}\int_{-\infty}^{\infty} dz e^{-izt}R_0(z-i\eta)\ (t>0), \tag{C2}$$

where $R_0(z-i\eta) = (z-H_0-i\eta)^{-1}$. We substitute this expression, perform the t' integral, and use $\frac{e^{izt}-1}{iz} = \pi\delta(z)$ for large t. Noting that $\mathcal{U}_0(t',t)$ corresponds to evolution backwards in time and corresponds to the complex conjugate of Eq. (C2), we have

$$\frac{d}{dt}|U_{fi}(t)|^2 = -\frac{1}{2i}\Omega^2|\langle f|S^-|i\rangle|^2\int_{-\infty}^{\infty}\frac{dz}{2\pi i}\langle f|R(z-i\eta)|f\rangle\langle i|R(z+E+i\eta)|i\rangle + \text{c.c.} \tag{C3}$$

We now incorporate the influence of vibrations on this result by inserting the vibration-induced self-energy in the resolvents [Eq. (26)],

$$\begin{aligned}\frac{d}{dt}|U_{if}(t)|^2 &= -\frac{1}{2i}\Omega^2|\langle f|S^-|i\rangle|^2\int_{-\infty}^{\infty}\frac{dz}{2\pi i}\frac{1}{z-E_f-\Sigma_f}\frac{1}{z-E-E_i-\Sigma_i^*} + \text{c.c.}\\ &= -\frac{1}{2i}\Omega^2|\langle f|S^-|i\rangle|^2\frac{1}{E_i+\Sigma_i'-E_f-\Sigma_f'-E+i(\Gamma_i+\Gamma_f)} + \text{c.c.}\\ &= \Omega^2|\langle f|S^-|i\rangle|^2\frac{\Gamma_i+\Gamma_f}{(E_i+\Sigma_i'-E_f-\Sigma_f'+E)^2+(\Gamma_i+\Gamma_f)^2},\end{aligned} \tag{C4}$$

where $\Sigma_{i,f} = \Sigma'_{i,f} + i\Gamma_{i,f}$ is the self-energy. Thus, we obtain Eq. (34).

[1] *Scalable Quantum Computers: Paving the Way to Realization*, edited by S. L. Braunstein and H.-K. Lo (Wiley-VCH, Berlin, 2001).

[2] A. J. Leggett, S. Chakravarty, A. T. Dorsey, M. P. A. Fisher, A. Garg, and W. Zwerger, Rev. Mod. Phys. **59**, 1 (1987).

[3] U. Weiss, *Quantum Dissipative Systems*, 2nd ed. (World Scientific, Singapore, 1999).

[4] R. H. Dicke, Phys. Rev. **93**, 99 (1954).

[5] I. Carusotto and C. Ciuti, Rev. Mod. Phys. **85**, 299 (2013).

[6] E. Sela, A. Rosch, and V. Fleurov, Phys. Rev. A **89**, 043844 (2014).
[7] R. Mottl, F. Brennecke, K. Baumann, R. Landig, T. Donner, and T. Esslinger, Science **336**, 1570 (2012).
[8] R. Landig, L. Hruby, N. Dogra, M. Landini, R. Mottl, T. Donner, and T. Esslinger, Nature (London) **532**, 476 (2016).
[9] H. J. Lipkin, N. Meshkov, and A. J. Glick, Nucl. Phys. **62**, 188 (1965).
[10] J. I. Latorre, R. Orús, E. Rico, and J. Vidal, Phys. Rev. A **71**, 064101 (2005).
[11] T. Opatrný, M. Kolář, and K. K. Das, Phys. Rev. A **91**, 053612 (2015).
[12] A. Russomanno, R. Fazio, and G. E. Santoro, Europhys. Lett. **110**, 37005 (2015).
[13] L. F. Santos and F. Pérez-Bernal, Phys. Rev. A **92**, 050101 (2015).
[14] J. Majer, J. M. Chow, J. M. Gambetta, J. Koch, B. R. Johnson, J. A. Schreier, L. Frunzio, D. I. Schuster, A. A. Houck, A. Wallraff, A. Blais, M. H. Devoret, S. M. Girvin, and R. J. Schoelkopf, Nature (London) **449**, 443 (2007).
[15] J. M. Fink, R. Bianchetti, M. Baur, M. Göppl, L. Steffen, S. Filipp, P. J. Leek, A. Blais, and A. Wallraff, Phys. Rev. Lett. **103**, 083601 (2009).
[16] J. Larson, Europhys. Lett. **90**, 54001 (2010).
[17] J. Klaers, J. Schmitt, F. Vewinger, and M. Weitz, Nature (London) **468**, 545 (2010).
[18] E. De Angelis, F. De Martini, and P. Mataloni, J. Opt. B **2**, 149 (2000).
[19] V. A. Yurovsky, Phys. Rev. A **93**, 023613 (2016).
[20] E. V. Goldstein and P. Meystre, Phys. Rev. A **56**, 5135 (1997).
[21] S. Zeeb, C. Noh, A. S. Parkins, and H. J. Carmichael, Phys. Rev. A **91**, 023829 (2015).
[22] I. G. Kaplan, *Symmetry of Many-Electron Systems* (Academic, London, 1975).
[23] W. Heitler, Z. Phys. **46**, 47 (1927).
[24] K. Hepp and E. Lieb, Ann. Phys. (N.Y.) **76**, 360 (1973); Y. K. Wang and F. T. Hioes, Phys. Rev. A **7**, 831 (1973).
[25] A. C. Hewson, *The Kondo Problem to Heavy Fermions* (Cambridge University Press, Cambridge, 1997).
[26] J. L. Skinner and D. Hsu, J. Phys. Chem. **90**, 4931 (1986).
[27] R. W. Ziolkowski, J. M. Arnold, and D. M. Gogny, Phys. Rev. A **52**, 3082 (1995).
[28] M. Sukharev and A. Nitzan, Phys. Rev. A **84**, 043802 (2011).
[29] E. G. Dalla Torre, Y. Shchadilova, E. Y. Wilner, M. D. Lukin, and E. Demler, arXiv:1608.06293.
[30] M. Ahsan Zeb, P. G. Kirton, and J. Keeling, arXiv:1608.08929.
[31] A. Shalabney, J. George, J. Hutchison, G. Pupillo, C. Genet, and T. W. Ebbesen, Nat. Comm. **6**, 5981 (2015).
[32] J. del Pino, J. Feist, and F. J. Garcia-Vidal, New J. Phys. **17**, 053040 (2015).
[33] A. Strashko and J. Keeling, Phys. Rev. A **94**, 023843 (2016).
[34] J. del Pino, J. Feist, and F. J. Garcia-Vidal, J. Phys. Chem. C **119**, 29132 (2015).
[35] V. A. Yurovsky, Phys. Rev. A **91**, 053601 (2015).
[36] V. A. Yurovsky, Phys. Rev. Lett. **113**, 200406 (2014).